

Tunable quantum dots in monolayer grapheneG. Giavaras¹ and Franco Nori^{1,2}¹*Advanced Science Institute, RIKEN, Wako-shi, Saitama 351-0198, Japan*²*Department of Physics, University of Michigan, Ann Arbor, Michigan 48109-1040, USA*

(Received 7 October 2011; revised manuscript received 9 April 2012; published 27 April 2012)

We examine a graphene quantum dot formed by combining an electric and a uniform magnetic field. The electric field creates a smooth quantum well potential while the magnetic field induces an exponential tail to the dot states. The states peak in the well and the electrostatic barrier region as a result of the Klein tunneling effect. Coupling between dot states which peak in different regions can be achieved with the electric and magnetic fields. The tunability of this dot with moderate external fields could be used for designing quantum devices in monolayer graphene.

DOI: [10.1103/PhysRevB.85.165446](https://doi.org/10.1103/PhysRevB.85.165446)

PACS number(s): 73.21.La, 73.23.-b, 81.05.ue

I. INTRODUCTION

The electronic properties of monolayer graphene are derived from a two-dimensional Dirac equation. This makes graphene suitable to explore quasirelativistic effects in condensed matter physics as well as attractive for quantum devices.¹ For these two reasons various graphene-based devices are under investigation. Lithographic confinement leading to quantum dot behavior has been achieved in nanocrystals of graphene with a diameter of some tens of nanometers. Coulomb blockade, single-electron transport, charge, and spin spectroscopy have been demonstrated in single and coupled dots.¹⁻⁴

Theoretical studies have shown that the electronic properties of the dots formed in nanocrystals depend crucially on the type of edges.¹ However, the edges cannot be routinely controlled experimentally, because edge disorder seems to be unavoidable and different types of edges may coexist in one sample. Forming dots in monolayer graphene is necessary in order to spatially isolate the dot states from the edges. In this case the fabrication of the dot involves the application of external fields. However, electrons in graphene are massless and via Klein tunneling can penetrate any electrostatic potential barrier.^{1,5} Consequently, pure electrostatic confinement in graphene is not possible⁶⁻⁹ and a uniform magnetic field has to be applied.⁹ The usual ease in tuning a dot electrically cannot be exploited in graphene, though an exception may occur for zero-energy states.¹⁰

As shown in this work, the physics of a graphene dot formed by combining an electric and a uniform magnetic field is rich and has great potential for manipulation and control over the dot system. The electric field creates a quantum well while the magnetic field induces an exponential tail to the quantum states which is needed for confinement. The electric field modifies the Landau level spectrum by inducing energy levels within the Landau gaps. These levels lie in a relatively low density of states. Here we demonstrate that the tunability of these levels can be achieved with both electric and magnetic fields.

The dot states exhibit features which arise due to the relativistic character of graphene. When the magnetic field is low, there is a class of states which peak in the quantum well region but have also a large oscillatory amplitude in the electrostatic barrier region due to Klein tunneling. As the field increases, the amplitude in the barrier decreases exponentially

and the states become confined very close to the center of the dot. The suppression of the Klein tunneling with the magnetic field may be employed in coupled dots. The interdot coupling is expected to be strong (weak) in the low (high) magnetic field regime. Strong interdot coupling seems to be possible even when the dots are separated by a long distance. There is also another class of states which peak mainly in the barrier region. These states can couple to states which have a large amplitude in the well, with a coupling strength that depends on the fields. Numerical calculations show that it should be experimentally possible to probe the dot properties in clean sheets of graphene.

The dot system studied here could allow the investigation of the Klein tunneling effect in a well-defined two-dimensional system. In nanocrystals of graphene, the geometry is not circularly symmetric and a spectral gap opening may prevent Klein tunneling from taking place. Moreover, the system that we study enables the formation and coupling of multiple graphene dots in various two-dimensional configurations. This may be more difficult to achieve using nanocrystals. The proposed dot could even be formed in suspended sheets of graphene in order to minimize interaction and disorder effects due to the substrate.

In Sec. II we show that some of the basic properties of the dot system can be extracted directly from the classical energy-momentum relation of massless particles. We also present the quantum mechanical model of the dot which is based on the Dirac equation for the envelope functions of graphene. Furthermore, in Sec. II a semianalytical model is solved for a piecewise constant quantum well potential. Calculations are presented in Sec. III, where the tunability of the dot with electric and magnetic fields is demonstrated. The conclusions of this work are given in Sec. IV.

II. GRAPHENE DOT FORMED BY ELECTRIC AND MAGNETIC FIELDS**A. Dot properties derived from the classical motion of massless particles**

Consider a graphene sheet in a vector potential $\mathbf{A} = (0, A_\theta, 0)$ and an electrostatic potential V , and for simplicity choose A_θ and V to have cylindrical symmetry. Here V defines a quantum well potential centered at $r = 0$ which is modeled

as $V(r) = -V_0 \exp(-r^2/d^2)$, with $V_0 \geq 0$. Also, A_θ generates a perpendicular magnetic field to the graphene sheet which, in this work, is chosen to be uniform, $\mathbf{B} = B\hat{z} = \nabla \times \mathbf{A}$, thus $A_\theta = Br/2$. The classical energy-momentum relation of a massless particle moving in the fields \mathbf{A} and V , with energy E and radial momentum p , is

$$v_F^2 p^2 = (E - V)^2 - v_F^2 \left(\frac{M}{r} + eA_\theta \right)^2, \quad (1)$$

where the term M/r is due to the angular motion and $v_F = 10^6 \text{ m s}^{-1}$ is the Fermi velocity in graphene. The classical motion is restricted to the region where $p^2 > 0$, and $p^2 = 0$ defines the classical turning points. The ability of the magnetic field to induce confined states with an exponential tail, regardless of momentum and energy, is based on the observation that if $A_\theta \neq 0$ then $p^2 < 0$ in the asymptotic regime of large r ($r \rightarrow \infty$). Therefore, classical motion is not allowed in this regime. But if $A_\theta = 0$, then asymptotically $p^2 > 0$ and classical motion is allowed, resulting in deconfined states with an oscillatory tail. In this work we are interested in the energy range $-V_0 < E < 0$ and confined states which are needed for quantum dots, henceforth $A_\theta \neq 0$.

Equation (1) shows that p^2 can take positive values even within the barrier region before it eventually becomes negative asymptotically.¹¹ For instance this can happen when $|E - V_0|$ is large and B is low. This regime can always be arranged by tuning the electric and magnetic fields. If $p^2 > 0$ in the barrier, then the quantum states are expected to have an oscillatory spatial dependence, a property which is related to the Klein tunneling effect for massless particles.^{5,12} In contrast, the states of a particle with mass described by a Schrödinger equation decay in the barrier.

Figure 1 shows $v_F^2 p^2$ together with the potential well. When $B = 0.3 \text{ T}$, then $p^2 > 0$ almost entirely in the barrier (well) region for $E = -30 \text{ meV}$ ($E = -8 \text{ meV}$), and hence the state is expected to be confined in the barrier (well). When $B = 0.05 \text{ T}$ and $E = -12 \text{ meV}$, then $p^2 > 0$ both in the well and barrier regions. In this case the state can have a large amplitude both in the well and the barrier. It can also be

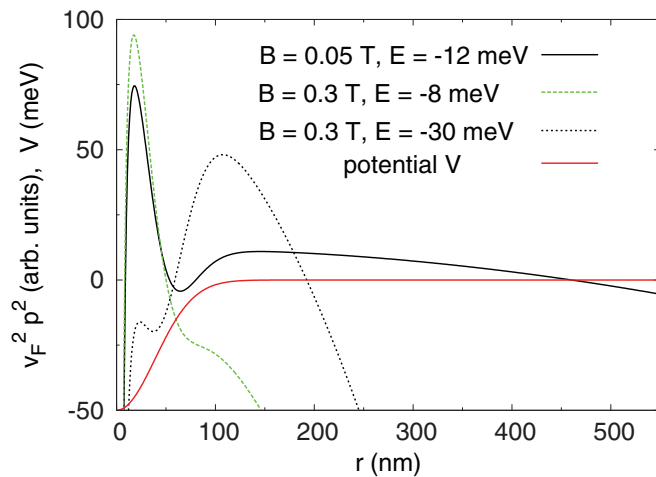


FIG. 1. (Color online) The figure shows $v_F^2 p^2$, defined in Eq. (1), as a function of the radial distance r for three choices of magnetic field B and energy E . The potential well V is also shown.

derived from Eq. (1) that if B is high enough and/or the angular momentum term is large ($M \gg 0$) then there exists an energy range for which $p^2 < 0$ for all r . So classical motion is not allowed, suggesting that quantum states do not exist in this range. Therefore, a gap, proportional to B and M , is formed in the energy spectrum. Then as the depth of the potential well increases the gap closes and states are formed in the well and/or barrier depending on the choice of energy.

Equation (1) provides some insight into the properties of the quantum dot and shows that different classes of states can be defined according to the region which the states tend to occupy. It also demonstrates the ability to tune at will the dot states with electric and magnetic fields. However, it cannot predict the energy levels of the dot and the exact pattern of the states. For this reason we present below the exact model of the quantum dot and identify its connection to the classical energy-momentum relation in Eq. (1).

B. Quantum mechanical dot model

In monolayer graphene there are two valleys that have to be considered, at the Dirac points K and K' , respectively, of the Brillouin zone.¹ In this work we assume that the two valleys are uncoupled, as it has been demonstrated in many experimental studies.¹ The physics is the same for both valleys; thus we examine the dot properties only for one valley. In the continuum approximation and for energies near the Dirac points, the two-component envelope functions Ψ satisfy a two-dimensional Dirac equation

$$[v_F \boldsymbol{\sigma} \cdot (\mathbf{p} + e\mathbf{A}) + V]\Psi = E\Psi, \quad (2)$$

where $\boldsymbol{\sigma}$ are the Pauli matrices, \mathbf{p} is the momentum operator, and E is the energy. For a circularly symmetric system, defined by the vector potential $\mathbf{A} = (0, A_\theta, 0)$ and the quantum well potential V of the previous subsection, we can write for the wave functions

$$\Psi = \frac{1}{\sqrt{r}} \begin{pmatrix} f_1(r) \exp[i(m-1)\theta] \\ i f_2(r) \exp(im\theta) \end{pmatrix}, \quad (3)$$

where $m = 0, \pm 1, \dots$ is the angular momentum number and r, θ are the radial distance and the azimuthal angle, respectively. The radial functions satisfy the equations¹³

$$V f_1 + \left(U + \gamma \frac{d}{dr} \right) f_2 = E f_1, \quad (4a)$$

$$\left(U - \gamma \frac{d}{dr} \right) f_1 + V f_2 = E f_2, \quad (4b)$$

with $v_F = \gamma/\hbar$ and

$$U = \gamma \frac{2m-1}{2r} + \gamma \frac{eA_\theta}{\hbar}. \quad (5)$$

This eigenvalue problem can be diagonalized numerically to give the eigenenergy E and the corresponding two-component eigenstate (f_1, f_2) . Here f_i gives the probability amplitude of finding an electron on one of the two sublattices of graphene.

Following the same method as that developed in Ref. 9, it can be shown that the state f_i satisfies the second-order

differential equation

$$\frac{d^2 f_i}{dr^2} + s(r) \frac{df_i}{dr} + w_i(r) f_i = 0, \quad (6)$$

with $s = V'/(E - V)$ and the prime denotes differentiation with respect to r . Also

$$w_i = -\frac{U^2}{\gamma^2} \pm \frac{U'}{\gamma} \pm s \frac{U}{\gamma} + \frac{(E - V)^2}{\gamma^2}, \quad (7)$$

where the minus (plus) sign is for $i = 1$ ($i = 2$). To derive a more familiar Schrödinger-like equation we eliminate the first derivative term. This can be done by writing f_i in the form

$$f_i = u_i \exp\left(-\frac{1}{2} \int s(r) dr\right), \quad (8)$$

and substituting Eq. (8) into Eq. (6). This procedure shows that the function u_i is a solution to the equation

$$\frac{d^2 u_i}{dr^2} + k_i^2(r) u_i = 0, \quad (9)$$

with

$$k_i^2 = \pm \frac{U'}{\gamma} \pm s \frac{U}{\gamma} - \frac{s'}{2} - \frac{s^2}{4} + \frac{v_F^2 p^2}{\gamma^2}, \quad (10)$$

where the minus (plus) sign is for $i = 1$ ($i = 2$). Unlike the coupled equations for f_i , the single equation for u_i has a more convenient form. The radial momentum p^2 in Eq. (1) can be directly identified in Eq. (10) with M replaced by $(m - 1/2)\hbar$. The quantum model through Eq. (9) suggests that the states are localized within the region where $k_i^2 > 0$. This region is defined not only by the $v_F^2 p^2$ term but also by the additional terms which appear in Eq. (10). Confined states, i.e., states that decay asymptotically, occur when $k_i^2(r \rightarrow \infty) \sim -v_F^2 e^2 A_\theta^2 < 0$, which is satisfied for $A_\theta \neq 0$. This condition agrees with that derived from Eq. (1).

One consequence of the Dirac equation is that the energy spectrum of the graphene dot is unbound. However, depending on the external fields, the energy levels and the quantum states can have simple patterns. For instance, when $V = 0$ and $m \geq 1$ the energy spectrum consists of two ladders (sets) of Landau levels (LLs) which can be determined analytically.¹⁴ The ladders are separated by a gap which is proportional to the field B and angular number m . The LLs are formed symmetrically with respect to $E = 0$ and the number of nodes in the corresponding Landau states increases successively by one for each new level in each energy ladder. For $m \leq 0$ one additional LL is formed at $E = 0$ for which one of the two components f_i is zero.

The inclusion of a potential term $V \neq 0$ modifies the spatial region where the Landau states are localized. In addition energy levels are formed within the Landau gaps. The simplest regime was studied in detail in Ref. 15 within an approximate model. It was shown there that for $m \geq 1$ the dot states are approximately localized in either of the two regions defined by the two terms $E - V \pm U$, which create two (independent) effective quantum wells. Each well contributes one ladder of energy levels to the dot spectrum. For $m \leq 0$ the two wells can no longer be defined because there is point at which the two curves $V \pm U$ cross. Nevertheless, exact numerical

calculations confirm the formation of the two ladders for $m \leq 0$ as well.¹⁶

The model developed in Ref. 15 is valid provided the two effective wells have no common energy range. This can be achieved when there is an energy gap between the minimum of $E - V + U$ and the maximum of $E - V - U$. If this condition is not satisfied the states of the two ladders can form a richer pattern. Specifically, when m is small the states of the upper ladder tend to couple to the states of the lower ladder. This regime is the main concern of the present work and it typically occurs when the potential depth V_0 is large and the field B is low. As shown below, the induced coupled states can have a large amplitude both near the center of the quantum well and in the barrier region. The coupling strength can be controlled at will by tuning the external fields and hence different classes of states can be probed. If m is large the states are not affected by the quantum well since they are localized in the asymptotic region where the potential is constant. As a result the states for large m behave as Landau states.

The formation of the two ladders and the coupling between the corresponding states have also been predicted theoretically in a graphene dot system at zero magnetic field but with a spatially modulated spectral (Dirac) gap in the energy dispersion.¹³ In this system the states are confined provided their energies lie inside the gap. The coupling strength can be tuned with the potential depth and the induced coupled states can be probed inside the spatial region where the spectral gap is zero.¹³

C. Dot formed by a piecewise-constant potential well and uniform magnetic field

This work is concerned with quantum dots formed in monolayer graphene by combining electric and magnetic fields. In this context, the simplest dot model that can be studied is when the magnetic field is uniform and the induced potential well is piecewise constant, e.g., $V(r) = -|v_0| \Theta(r - R)$, where $|v_0|$ is the depth of the well, R is its radius, and Θ is the step function. For completeness the method to solve this problem is outlined here, though the reader can proceed directly to Sec. III. As in Sec. II B Eqs. (4a) and (4b) are uncoupled and a second-order differential equation is derived for each radial state f_i . Equation (6) for $s = 0$ gives

$$\frac{d^2 f_i}{dr^2} + \frac{(E - V)^2}{\gamma^2} f_i - \frac{U^2}{\gamma^2} f_i \pm \frac{1}{\gamma} \frac{dU}{dr} f_i = 0. \quad (11)$$

This equation is written in the more convenient form

$$\frac{d^2 f_i}{dr^2} - \frac{a^2 r^4 + b_i r^2 + c_i}{r^2} f_i = 0, \quad (12)$$

with the coefficients $a = eB/2\hbar$ and

$$b_1 = \frac{meB}{\hbar} - \frac{(E - V)^2}{\gamma^2}, \quad c_1 = (m - 1)^2 - \frac{1}{4}, \quad (13a)$$

$$b_2 = \frac{(m - 1)eB}{\hbar} - \frac{(E - V)^2}{\gamma^2}, \quad c_2 = m^2 - \frac{1}{4}. \quad (13b)$$

The form of Eq. (12) reveals that the states f_i can be expressed with the help of the confluent hypergeometric functions \mathcal{U} and \mathcal{M} (Ref. 17). For example, when $m \geq 1$ the two-component

state which is regular at the origin and decays asymptotically has for $r \leq R$ the form

$$\begin{pmatrix} f_1 \\ f_2 \end{pmatrix} = \eta e^{-ar^2/2} \begin{pmatrix} r^{d_1} \mathcal{M}(A_1, B_1, ar^2) \\ c_0 r^{d_2} \mathcal{M}(A_2, B_2, ar^2) \end{pmatrix}, \quad (14)$$

with

$$c_0 = \frac{2\gamma a}{E + |v_0|} \left(1 - \frac{A_1}{B_1} \right). \quad (15)$$

For $R \leq r$ the two-component state has the form

$$\begin{pmatrix} f_1 \\ f_2 \end{pmatrix} = \beta e^{-ar^2/2} \begin{pmatrix} r^{d_1} \mathcal{U}(A_1, B_1, ar^2) \\ g_0 r^{d_2} \mathcal{U}(A_2, B_2, ar^2) \end{pmatrix}, \quad (16)$$

with

$$g_0 = \frac{2\gamma a}{E}. \quad (17)$$

The auxiliary parameters are

$$d_i = \frac{1 + \sqrt{4c_i + 1}}{2}, \quad (18a)$$

$$A_i = \frac{b_i}{4a} + \frac{1}{2} \left(\frac{1}{2} + d_i \right), \quad (18b)$$

$$B_i = \frac{1}{2} + d_i. \quad (18c)$$

The corresponding energies can be obtained from a standard matching condition which requires that both f_1 and f_2 to be continuous at $r = R$. This condition leads to an algebraic equation for the energies which is solved numerically. Then having calculated the energies and taking also into account the normalization condition the ratio β/η is determined. Some quantum states for $m = +1$ are plotted in Fig. 2. The region in which the states peak depends on the magnetic field and energy. This behavior is consistent with that derived from the energy-momentum relation in Eq. (1).

III. TUNING THE GRAPHENE DOT WITH ELECTRIC AND MAGNETIC FIELDS

In any real sample of graphene a piecewise-constant potential well cannot be generated. So a more realistic choice is made for the potential well and, specifically, the potential well is chosen to have a Gaussian form as in Sec. II A with $d = 55$ nm. Numerical calculations of the electrostatic potential in the graphene sheet confirm that the Gaussian potential is a very good approximation to the potential that is generated by gate electrodes or a scanning tunneling microscope tip.⁹ Also, the Gaussian potential produces a smooth spatial variation on the scale of the lattice constant and hence intervalley scattering can be ignored.

The results presented in this work are for the $m = +1$ states which can peak very close to the center of the potential well and thus can be considered as quantum dot states. States with small values of m show similar trends to those with $m = +1$. As m increases, the states become localized in the asymptotic region where the potential is constant and hence the effect of the quantum well on the states becomes negligible. This property also occurs for a repulsive potential profile.¹⁸ Therefore, in the large- m regime the corresponding quantum

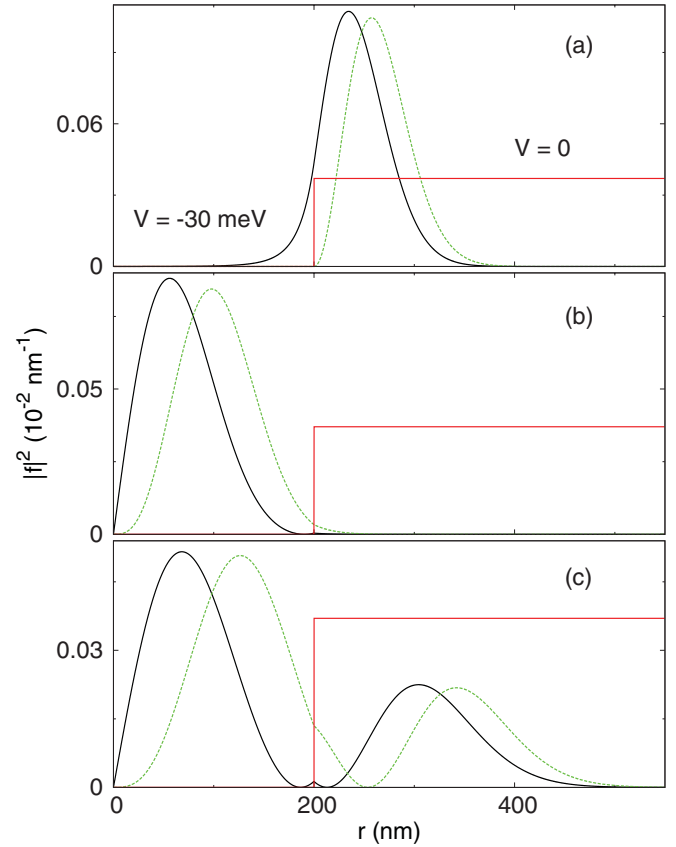


FIG. 2. (Color online) Quantum states for $m = +1$ and a piecewise-constant potential well which has a radius $R = 200$ nm and depth $|v_0| = 30$ meV. The magnetic field B and the energy E are (a) $B = 0.2$ T, $E \approx -29.6$ meV, (b) $B = 0.09$ T, $E \approx -13.9$ meV, and (c) $B = 0.09$ T, $E \approx -18.1$ meV. Solid (dashed) curves show $|f_1|^2$ ($|f_2|^2$).

states are described approximately by Landau states since only the vector potential and angular momentum are important.

The dot states of interest have to be energetically isolated from other states; that is, they have to lie in a region of low density of states (DOS), in order to be detectable. If this condition is satisfied then scanning tunneling microscopy (STM) could be used to probe the local density of states and features of individual quantum states. When there is no potential variation and a perpendicular magnetic field is applied to a graphene sheet the DOS is high at the LLs which form the energy spectrum¹⁴ $\mathcal{E}_N = \pm \sqrt{2\hbar v_F^2 B N}$, with $N = n + (m + |m|)/2$, and n being the radial quantum number. A potential well induces energy levels within the Landau gaps where the DOS can be low enough. As the external field is tuned, the dot levels of interest have to lie within a specific Landau gap so that their detection to be possible. For this reason we focus on dot levels which lie between the first few LLs, for which the Landau gaps are larger compared to those of highly excited LLs.

We assume that for the low magnetic fields considered in this work there is no overlap between the LLs. Any LL broadening, for example, due to disorder and interaction effects,^{19,20} is small and it is typically less than ~ 2 meV. It may be possible to achieve this condition in clean samples

of graphene. In particular, experiments in suspended sheets of graphene have measured very large mobilities indicating that these sheets are less sensitive to disorder and impurities introduced by the substrate.^{21,22}

A. Electric field effect on the dot

As discussed in Sec. II B, in the graphene dot system formed by electric and magnetic fields, the energy levels for a fixed value of m can form two energy ladders separated by a gap.¹⁶ This configuration can be achieved for a high magnetic field and a small well depth. When the well depth increases, energy levels from the upper energy ladder fall in the gap, while the corresponding states develop a large amplitude in the well region. Eventually, when the well depth is large, states which peak in the well couple to states of the lower energy ladder, and this behavior is manifested in the energy diagram by the formation of anticrossing points.²³

To demonstrate these effects, we show in Fig. 3 the energy diagram as a function of the potential depth V_0 for a magnetic field $B = 0.1$ T. For $V_0 = 0$ the energy levels correspond to the LLs of a graphene sheet. For a small V_0 , the energy levels which define the two energy ladders emerge into the Landau gaps. When $V_0 \sim 0$ these levels are separated by a gap which is approximately equal to the energy splitting between the LLs $+1$ and -1 (Ref. 24). As V_0 increases, the gap closes and eventually energy levels of the upper ladder anticross with energy levels of the lower ladder. The general trend is that if the magnetic field is low the gap between the two energy ladders is small and therefore the anticrossing points appear for a small well depth V_0 . For instance, the first anticrossing point at $B = 0.1$ T is formed for $V_0 \approx 63$ meV (see Fig. 3), while at $B = 0.2$ T for $V_0 \approx 73$ meV. With a further increase of V_0 , a state of the lower energy ladder couples successively to states with higher energy in the well, forming a series of anticrossing points. Thus the required variation of V_0 to probe two successive anticrossing points becomes smaller as the typical energy splitting in the well decreases.

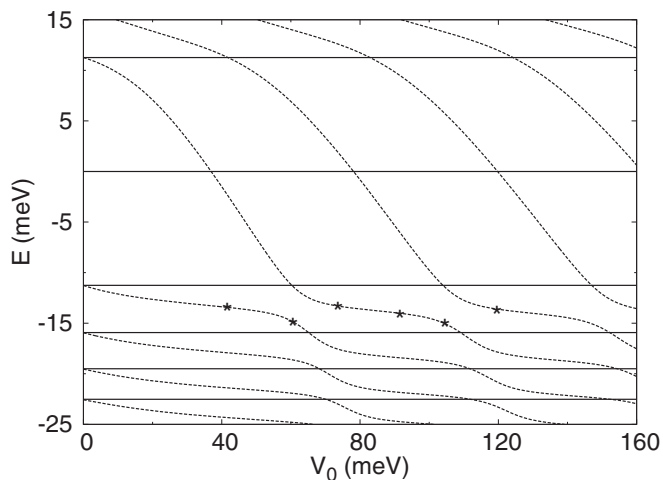


FIG. 3. Energy levels (dashed curves) as a function of the potential depth V_0 , for $m = +1$ and a magnetic field $B = 0.1$ T. Some Landau levels are also shown (horizontal solid lines). The quantum states for the marked energies are shown in Fig. 4.

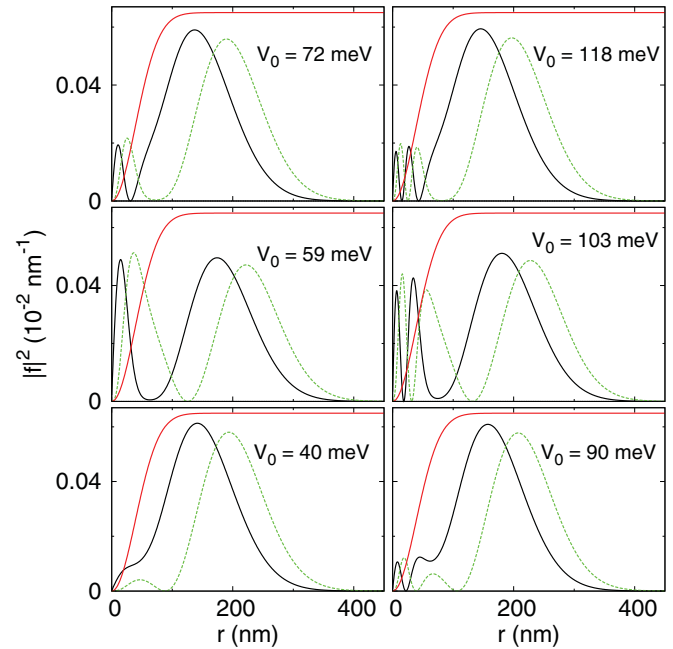


FIG. 4. (Color online) Quantum states for the marked energies shown in Fig. 3. The potential depth is V_0 . Solid (dashed) curves show $|f_1|^2$ ($|f_2|^2$). The potential well (in arbitrary units) is also shown.

Here we focus on the state with the highest energy in the lower ladder and its coupling to quantum well states. This state corresponds for $V_0 = 0$ to the LL -1 and then for $V_0 \neq 0$ the coupling leads to a “hybridized” state with energy between the LLs -1 and -2 . Some examples of this hybridized state are shown in Fig. 4. Comparison of the states in the left panels with those in the right panels shows that the number of nodes for each radial component increases by one in the well region¹¹ $r \lesssim 80$ nm, when a new anticrossing point is formed in the energy diagram (Fig. 3). This happens because for each new anticrossing point a higher energy state in the well is involved which typically has an extra node. Near the anticrossing points the coupling is strong and hence the amplitude of each state in the well region is large. This occurs, for example, for $V_0 = 59$ meV and 103 meV. Away from the anticrossing points the coupling is weak and the amplitude of the states in the well decreases, e.g., for $V_0 = 40$ meV and 90 meV.

As seen in Fig. 4, the hybridized state has a peak in the barrier region¹¹ which, to a good approximation, is insensitive to V_0 . The reason is that the charge carriers in graphene are massless and they exhibit Klein tunneling. This allows the states to develop an oscillatory amplitude in the barrier. In conventional dots obeying Schrödinger’s equation the quantum states decay in the barrier. Klein tunneling takes place in the two-dimensional graphene dot when within a barrier region $k_i^2 > 0$ in Eq. (10). This condition can be arranged easily for the dot system by tuning the external fields. Furthermore, the exact pattern of the state in the barrier depends on the choice of energy. Specifically, the number of peaks within the barrier increases for states which lie between higher excited LLs with $\mathcal{E}_N < 0$. However, the narrowing of the corresponding Landau gaps in combination with the expected broadening of the LLs in any real sample of graphene may make the detection of these states difficult.

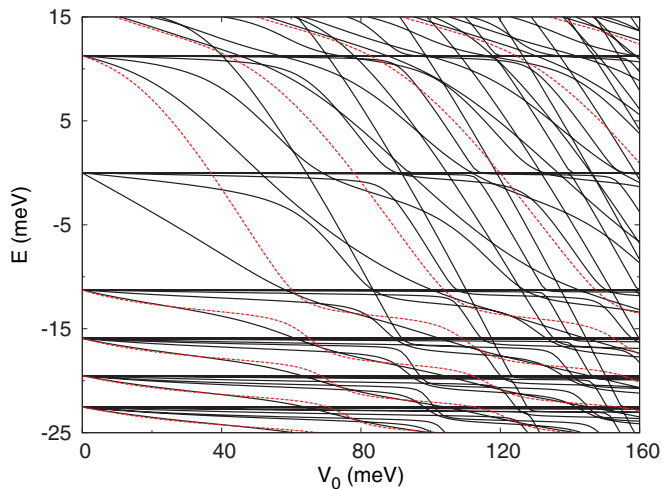


FIG. 5. (Color online) Energy diagram of the graphene dot as a function of the potential depth V_0 , for a magnetic field $B = 0.1$ T. The horizontal lines correspond to the Landau levels which are independent of V_0 . The dotted lines are the energy levels for $m = +1$.

Figure 5 illustrates the energy diagram of the dot as a function of the potential depth V_0 . Here all possible values of m are taken into account, but as explained above, for a large m the corresponding energy levels behave as LLs and thus they have the dependence $\mathcal{E}_N \propto -\sqrt{BN}$. Between the LLs there are regions where only a few levels lie, suggesting that the corresponding states could be probed with STM measurements.²⁵ For this reason the energy of the hybridized state in Fig. 4 is adjusted between the LLs -1 and -2 where the DOS is relatively low. Inspection of Fig. 5 shows that there are ranges of V_0 in which the energy of this state is at least 0.5 meV away from any other energy levels. Thus it should be experimentally possible to probe the pattern of the state in Fig. 4 in clean samples of graphene with a small broadening of the LLs. The local DOS near the center of the dot is expected to show a low-high-low variation as V_0 sweeps through an anticrossing point.

When the broadening of the LLs is large, the regions of low DOS which occur between the LLs shrink making the detection of individual dot states difficult; the states have to lie in a very narrow energy range (window) in order to be detectable. A high magnetic field B may increase this energy range provided that any broadening of the LLs increases much slower than the Landau gaps. However, when B is high a large V_0 is needed for anticrossing points to appear and the states to follow the pattern in Fig. 4. In this case the disadvantage is that the DOS between the LLs increases as V_0 and B increase, suggesting that the magnetic field cannot be chosen arbitrarily high. Also, if in an experiment it is desirable for the state to peak in the barrier region and far from the center of the dot then the magnetic field has to be kept low.

In order to deal with the broadening of the LLs it may be necessary to probe hybridized states between the LLs 0 and -1 , for which the Landau gap is the largest. Though, only states with $m \leq 0$ can, for certain parameter regimes, form anticrossing points at energies which lie between the LLs 0 and -1 . This can be understood from the fact that for $V_0 = 0$ only states with $m \leq 0$ contribute to the zeroth Landau level.

Then as V_0 increases, their energies emerge into the zeroth Landau gap and eventually anticross with energy levels of the upper ladder. States with $m \leq 0$ can also form anticrossing points in excited Landau gaps as happens with the $m = +1$ states in Fig. 3.

B. Magnetic field effect on the dot

The effect of a magnetic field on the dot is now examined when the potential well is fixed. In Sec. III A it was shown that, when the electric field increases, states belonging to different energy ladders become coupled. Moreover, the coupling is strong near the anticrossing points. In this section it is demonstrated that when the magnetic field increases the coupling is suppressed resulting in states which correspond approximately to individual states in each ladder.

In Fig. 6 the energy diagram is plotted as a function of the magnetic field when the depth of the potential well is $V_0 = 51$ meV. We are interested in the two highest energy levels below zero (for $m = +1$) which are denoted by E_1 and E_2 . In the field range $0.04 < B < 0.5$ T, the E_1 level lies between the LLs 0 and -1 , while for $0.04 < B < 0.35$ T the E_2 level lies between the LLs -1 and -2 . Thus quantum states can be arranged to lie between successive LLs in a wide field range. Calculations show that this effect is robust and can be achieved for different well depths and m values. In addition, as shown below within a specific magnetic field range the spatial region in which the states are localized changes drastically, confirming that the tunability of the dot is feasible with a uniform magnetic field.

Figure 7(a) shows the quantum state corresponding to the energy level E_2 in Fig. 6. This ‘‘hybridized’’ state is formed due to the coupling between the states of the two energy ladders. In particular, the peak in the well (barrier) region¹¹ is due to the state in the upper (lower) ladder. When $B = 0.04$ T the coupling is strong and the hybridized state peaks both in the well region, that is $r \lesssim 80$ nm, and the barrier.²⁶ As B increases, the coupling is suppressed and the amplitude of the hybridized state very close to the center of the well decreases.

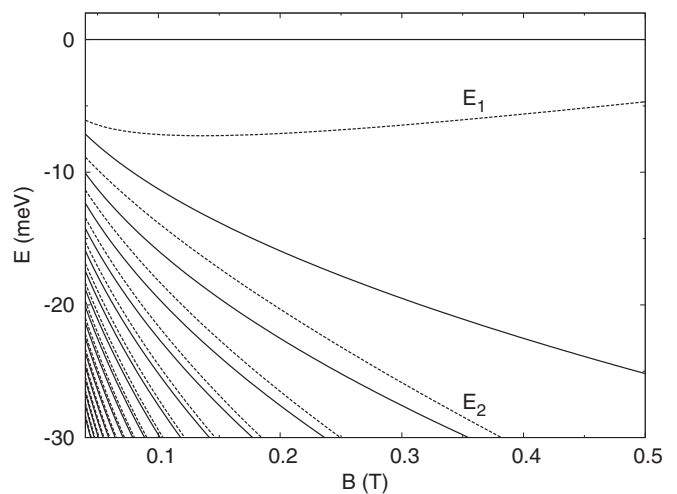


FIG. 6. Energy levels (dashed curves) as a function of the magnetic field B , for $m = +1$ and a potential depth $V_0 = 51$ meV. Some Landau levels are also shown (solid curves). The quantum states for the energy levels $E_{1,2}$ are shown in Fig. 7.

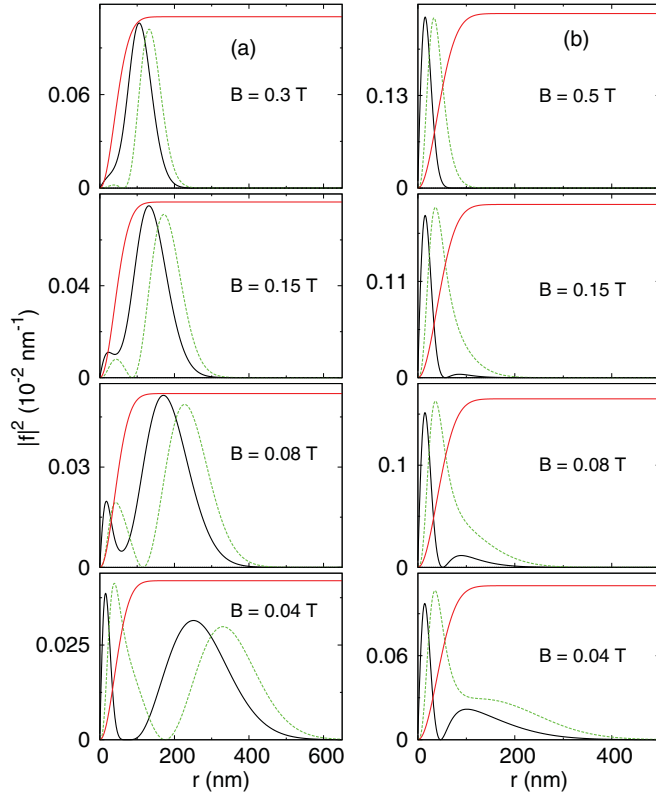


FIG. 7. (Color online) Quantum states for the energies shown in Fig. 6. For the energy level (a) E_2 and (b) E_1 . Solid (dashed) curves show $|f_1|^2$ ($|f_2|^2$). The potential well (in arbitrary units) is also shown.

Consequently, the hybridized state takes approximately the form of the state in the lower energy ladder. Also, when the field increases the magnetic confinement becomes stronger; therefore the state in the lower ladder shifts closer to the center of the dot and becomes localized in a narrower region. These trends are also displayed by the hybridized state in Fig. 7(a), which has a large peak in the region $200 \lesssim r \lesssim 400$ nm at $B = 0.04$ T, whereas the peak occurs around $50 \lesssim r \lesssim 150$ nm at $B = 0.3$ T.

The magnetic-field-dependent coupling is also responsible for the behavior of the “hybridized” state corresponding to the energy level E_1 [see Fig. 7(b)]. At $B = 0.04$ T the state peaks in the well region $r \lesssim 80$ nm, but has also a large amplitude in the barrier region before it eventually decays asymptotically. Klein tunneling is involved in the low field regime but is not so pronounced because there is only a small region with $k_i^2 > 0$ within the barrier. Then as B increases the amplitude of the two components in the barrier is gradually suppressed and the state becomes confined near the center of the well. For $B = 0.5$ T the hybridized state has approximately the form of the state in the upper energy ladder and $k_i^2 < 0$ everywhere in the barrier. Thus no Klein tunneling occurs at high B . The regime of high magnetic field as well as the symmetry between a dot and an antidot system have been investigated theoretically in Ref. 27. A graphene dot system especially designed to probe the Klein tunneling effect in a two-dimensional geometry has been studied in Ref. 9.

Figure 7 demonstrates that the magnetic-field-induced suppression of the amplitude of the states in the barrier is a

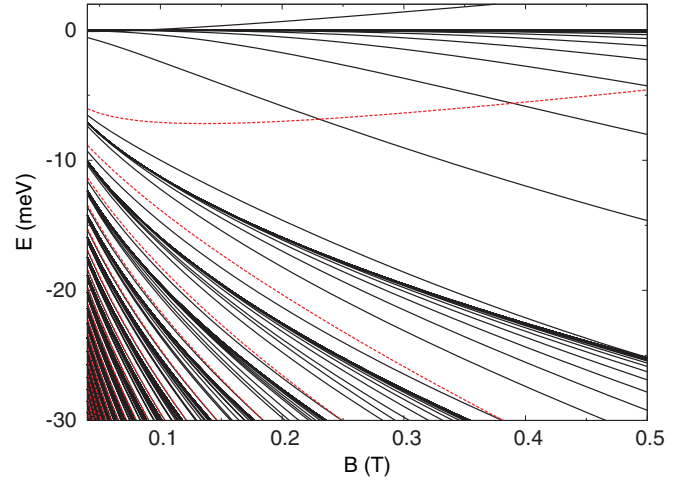


FIG. 8. (Color online) Energy diagram of the graphene dot as a function of the magnetic field B , for a potential depth $V_0 = 51$ meV. The high-density regions have the same magnetic field dependence as that of the Landau levels in graphene ($\mathcal{E}_N \propto -\sqrt{BN}$). The dotted lines are the energy levels for $m = +1$.

strong effect. This property may be useful for a system of two neighboring graphene dots separated by a long distance. In this system the interdot coupling can be tuned with the magnetic field instead of using gate electrodes as in conventional dots. The coupling is expected to be strong in the low-field regime, provided Klein tunneling is involved. The coupling can be strong even when the two dots are far apart, a situation that cannot be arranged easily in conventional semiconductor dots.

In Fig. 8 we show the energy diagram of the dot as a function of the magnetic field B . All values of m are taken into account, but as explained above, when m is large the energy levels have the LL dependence $\mathcal{E}_N \propto -\sqrt{BN}$. As seen in Fig. 8, regions of very low DOS are formed between the lowest LLs. This condition can be arranged when the quantum well is narrow enough so that only a limited number of m values contributes energy levels between the LLs. The energy level E_1 in Fig. 6 crosses some other levels for a few values of B but it is isolated from any other levels in a wide field range. This property makes possible the resolution of the corresponding state and its variation with the magnetic field [Fig. 7(b)]. Investigation of the energy diagram in Fig. 8 shows that for $0.04 < B < 0.3$ T the energy level E_2 in Fig. 6 is at least 0.4 meV away from any other levels. This suggests that the corresponding quantum state [Fig. 7(a)] could be detected using STM measurements similar, for example, to those in Ref. 25.

To demonstrate the formation of confined states in a graphene quantum dot the main focus of the experiment should be on the state with energy level E_1 and in the field range $0.15 \lesssim B \lesssim 0.36$ T. The reason for this choice is twofold. First, this state lies in a very low DOS region and thus it could be resolved using standard charge sensing measurements. Second, the energy of this state is away from the LLs and its detection should be possible when the LL broadening is $\lesssim 10$ meV. This value has to be smaller when the magnetic field is not in the above range or when the experiment probes the energy level E_2 .

IV. DISCUSSION AND CONCLUSION

This work investigated the properties of a graphene quantum dot formed by the combination of electric and magnetic fields. The electric field creates a smooth quantum well potential which could be generated using gate electrodes. Because of the Klein tunneling effect in graphene the well cannot confine electrons. However, when a uniform magnetic field is applied perpendicular to the graphene sheet the states decay asymptotically as needed for confinement. The electric field modifies the Landau level spectrum by inducing levels within the Landau gaps. It was demonstrated that the states which correspond to these levels are tunable with the electric and magnetic fields. This property has also been considered in one-dimensional systems of graphene such as wave guides and wires.^{28,29}

Some of the basic properties of the dot system were qualitatively extracted from the classical energy-momentum relation of massless particles. These properties were then confirmed and quantified with exact numerical calculations. It was found that some states can peak both in the potential well and within the barrier because of the Klein tunneling effect in graphene. This behavior cannot be observed in a nonrelativistic dot described by a Schrödinger equation. States which peak in the barrier region occur also in one-dimensional systems of graphene and have been examined in Refs. 30 and 31.

The relative amplitude of the states in each region depends on the values of the electric and magnetic fields and thus it can be tuned at will. For example, at a high magnetic field there are states which peak very close to the center of the well and decay exponentially in the barrier. For low enough fields, Klein tunneling is involved and the amplitude of the states in the barrier increases drastically. Coupling between states which peak in different regions results in the formation of anticrossing points in the energy spectrum of the dot, provided the quantum well is deep. Numerical calculations suggest that the density of states is relatively low between the few lowest Landau levels. Therefore, it should be experimentally possible to probe individual quantum states when the broadening of the Landau levels is small.

ACKNOWLEDGMENTS

We thank P. A. Maksym, Y. Bliokh, V. Freilikher, and A. Rozhkov for comments on the manuscript. G.G. acknowledges support from the Japan Society for the Promotion of Science (JSPS). F.N. is partially supported by the ARO, NSF grant No. 0726909, JSPS-RFBR contract No. 12-02-92100, Grant-in-Aid for Scientific Research (S), MEXT Kakenhi on Quantum Cybernetics, and the JSPS via its FIRST Program.

¹A. V. Rozhkov, G. Giavaras, Y. P. Bliokh, V. Freilikher, and F. Nori, *Phys. Rep.* **503**, 77 (2011).

²C. Stampfer, J. Guttinger, F. Molitor, D. Graf, T. Ihn, and K. Ensslin, *Appl. Phys. Lett.* **92**, 012102 (2008).

³F. Molitor, S. Droscher, J. Guttinger, A. Jacobsen, C. Stampfer, T. Ihn, and K. Ensslin, *Appl. Phys. Lett.* **94**, 222107 (2009).

⁴J. Guttinger, T. Frey, C. Stampfer, T. Ihn, and K. Ensslin, *Phys. Rev. Lett.* **105**, 116801 (2010).

⁵M. I. Katsnelson, K. S. Novoselov, and A. K. Geim, *Nature Phys.* **2**, 620 (2006).

⁶A. Matulis and F. M. Peeters, *Phys. Rev. B* **77**, 115423 (2008).

⁷P. Hewageegana and V. Apalkov, *Phys. Rev. B* **77**, 245426 (2008).

⁸H.-Yi Chen, V. Apalkov, and T. Chakraborty, *Phys. Rev. Lett.* **98**, 186803 (2007).

⁹G. Giavaras, P. A. Maksym, and M. Roy, *J. Phys.: Condens. Matter* **21**, 102201 (2009).

¹⁰C. A. Downing, D. A. Stone, and M. E. Portnoi, *Phys. Rev. B* **84**, 155437 (2011).

¹¹The (electrostatic) barrier region is defined for $r > r_0$ and the well for $r < r_0$, where r_0 satisfies $V(r_0) = E$. The actual region where the state is confined depends not only on the external potential V but also on the angular momentum and the magnetic barrier due to the vector potential.

¹²A. Calogerakos and N. Dombey, *Contemp. Phys.* **40**, 313 (1999).

¹³G. Giavaras and F. Nori, *Appl. Phys. Lett.* **97**, 243106 (2010); *Phys. Rev. B* **83**, 165427 (2011).

¹⁴J. W. McClure, *Phys. Rev.* **104**, 666 (1956).

¹⁵G. Giavaras, P. A. Maksym, and M. Roy, *Physica E* **42**, 715 (2010).

¹⁶For $m \leq 0$ there is an additional energy level which lies in the gap.

¹⁷M. Abramowitz and I. A. Stegun, editors, *Handbook of Mathematical Functions* (Dover Publications, New York, 1965).

¹⁸P. S. Park, S. C. Kim, and S.-R. Eric Yang, *Phys. Rev. B* **84**, 085405 (2011).

¹⁹C. H. Yang, F. M. Peeters, and W. Xu, *Phys. Rev. B* **82**, 075401 (2010).

²⁰A. Pound, J. P. Carbotte, and E. J. Nicol, *Phys. Rev. B* **84**, 085125 (2011).

²¹K. I. Bolotin, K. J. Sikes, Z. Jiang, M. Klima, G. Fudenberg, J. Hone, P. Kim, and H. L. Stormer, *Solid State Commun.* **146**, 351 (2008).

²²X. Du, I. Skachko, A. Barker, and E. Y. Andrei, *Nature Nanotechnology* **3**, 491 (2008).

²³For some values of m anticrossing points are also formed in the upper energy ladder but not in the energy range of interest.

²⁴The notation here implies that the Landau level $+1$ has energy $+\sqrt{2e\hbar v_F^2 B}$, the Landau level -1 has energy $-\sqrt{2e\hbar v_F^2 B}$, and so on for the higher levels.

²⁵D. L. Miller, K. D. Kubista, G. M. Rutter, M. Ruan, W. A. de Heer, M. Kindermann, P. N. First, and J. A. Stroscio, *Nature Phys.* **6**, 811 (2010).

²⁶If the magnetic field is low, the state in the lower energy ladder peaks mainly in the barrier region and has a small amplitude in the well region. When the field increases, the amplitude in the well increases.

²⁷P. A. Maksym, M. Roy, M. F. Cracium, M. Yamamoto, S. Tarucha, and H. Aoki, *J. Phys.: Conf. Ser.* **245**, 012030 (2010).

- ²⁸Y. P. Bliokh, V. Freilikher, S. Savel'ev, and F. Nori, *Phys. Rev. B* **79**, 075123 (2009).
- ²⁹Y. P. Bliokh, V. Freilikher, and F. Nori, *Phys. Rev. B* **81**, 075410 (2010).

- ³⁰V. A. Yampol'skii, S. Savel'ev, and F. Nori, *New J. Phys.* **10**, 053024 (2008).
- ³¹J. M. Pereira Jr., F. M. Peeters, and P. Vasilopoulos, *Phys. Rev. B* **75**, 125433 (2007).